Soft robotic shorts improve outdoor walking efficiency in older adults

Enrica Tricomi[1*], Francesco Missiroli[†1], Michele Xiloyannis[†2], Nicola Lotti[1], Xiaohui Zhang[1], Marios Stefanakis[3,4], Maximilian Theisen[5], Jürgen Bauer[3,4], Clemens Becker[3,4] and Lorenzo Masia[1]

[1]Institut für Technische Informatik (ZITI), Heidelberg University, Heidelberg, Germany.
[2]Akina AG, Zürich, Switzerland.
[3]Digital Unit, Center for Geriatric Medicine, Heidelberg University Hospital, Heidelberg, Germany.
[4]Network Aging Research, Heidelberg University, Heidelberg, Germany.
[5]Psychological Institute, Heidelberg University, Heidelberg, Germany.

*Corresponding author. E-mail: enrica.tricomi@ziti.uni-heidelberg.de;
Contributing authors: † These authors contributed equally to this work;

SUPPLEMENTARY INFORMATION

This PDF file includes

1. Model for tendons displacement during walking
2. WalkON controller pseudocode
3. WalkON design: a comparative study on two hardware configurations in young adults hiking

Other Supplementary material

1. CAD files
2. Bill of Materials
3. Recorded data and scripts for analyses
4. Video accompanying the paper

Model for tendons displacement during walking

The displacement of artificial tendons in *WalkON* is controlled based on the kinematics of the hip joint and its progression throughout the gait cycle.

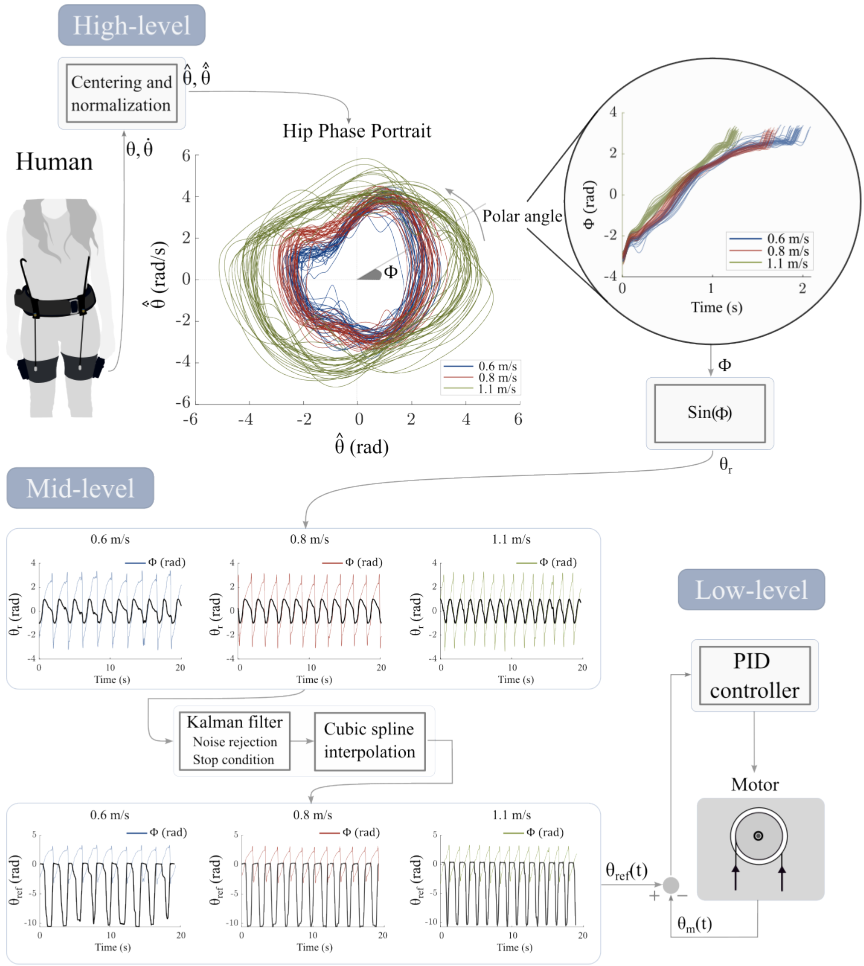

Fig. 1 Schematic representation of the control algorithm for *WalkON*. The control algorithm, illustrated with input signals and the corresponding processed outputs for three exemplary walking speeds, enables control of the artificial tendons by processing hip joint kinematic inputs and translating them into a reference trajectory for the actuator. At the high-level, the controller maps the circular motion of the hip joint's position and velocity, as presented in the hip phase portrait. From this mapping, it extracts a linearly increasing variable, which represents the gait phase, from the angle between the hip position and velocity during each step. At the mid-level, the controller employs a Kalman filter to enhance the signal's robustness against sensor noise. Subsequently, it generates a reference position trajectory for the actuator using cubic spline interpolation. Finally, the low-level controller manages feedback positioning of the artificial tendons.

The control algorithm analyzes motion information to generate a consistent motor actuator reference trajectory. This algorithm is composed of three layers, responsible for estimating the gait phase from kinematic data, generating the actuator reference motion based on the user's gait phase, and controlling the actuators (Fig. 1).

High-level controller A monotonically increasing gait phase variable is reconstructed from a single inertial sensor on each leg, measuring the hip angle $\theta(t)$ and the hip velocity $\dot{\theta}(t)$ in the sagittal plane. The polar angle between the two quantities is an indication of the progression of the gait phase, $\phi(t)$, along the gait cycle and is computed through the following equation, presented in the Iverson bracket notation:

$$\phi(t) = atan\left(\frac{\dot{\hat{\theta}}(t)}{\hat{\theta}(t)}\right)[\hat{\theta}(t) \neq 0] + \eta(t); \tag{1}$$

where $\hat{\theta}(t)$ and $\dot{\hat{\theta}}(t)$ are the hip angular position and velocity after normalization and centering; $\eta(t)$ is a corrective factor that takes into account that for each value of $\theta(t)$ there are at least two solutions due to the back and forth movement. The correct value of $\phi(t)$ can be disambiguated by summing the *sign* function of the hip angular velocity; then $\eta(t)$ is defined as:

$$\eta(t) = sgn(\dot{\hat{\theta}}(t))\left(\pi[\hat{\theta}(t) < 0] + \frac{\pi}{2}[\hat{\theta}(t) = 0]\right) \tag{2}$$

For the centering and normalization of $\theta(t)$ and $\dot{\theta}(t)$ we adopted a method based on Quintero et al.[1]: for each step, both variables are shifted about the origin of the hip phase portrait and $\theta(t)$ is re-scaled to match the amplitude of $\dot{\theta}(t)$:

$$\hat{\theta}(t) = \frac{|\dot{\theta}_{max_i}(t) - \dot{\theta}_{min_i}(t)|}{|\theta_{max_i}(t) - \theta_{min_i}(t)|}\Big(\theta(t) - \frac{\theta_{max_i}(t) + \theta_{min_i}(t)}{2}\Big) \tag{3}$$

$$\dot{\hat{\theta}}(t) = \dot{\theta}(t) - \frac{\dot{\theta}_{max_i}(t) + \dot{\theta}_{min_i}(t)}{2} \tag{4}$$

where the maximum and minimum values of $\theta(t)$ and $\dot{\theta}(t)$ are related to the i^{th} stride and are identified as the times in which the derivative of the signals, $\dot{\theta}(t)$ and $\ddot{\theta}(t)$ respectively, crosses the zero. These steps are needed to make the walking limit cycle as circular as possible, thus increasing the linearity of $\phi(t)$ in each stride. Finally, $\phi(t)$ is transformed into $sin(\phi(t))$ to approximate the sinusoidal-like behaviour of the hip joint in the sagittal plane. This signal is referred to as $\theta_{\mathrm{r}}(t)$ and lays the foundation for the derivation of the motor reference motion.

Mid-level controller The gait phase extraction method implemented at the High-Level shows high sensitivity to the noise captured from the inertial sensors (e.g., during heel strike at sustained speed or due to shifting movements of the textile frame on the user's thigh), that transfer to the motor reference motion signal $\theta_{\mathrm{r}}(t)$. Therefore, in order to increase the robustness of the control strategy to noise, we implemented a Kalman Filter[2] in cascade to the gait phase estimator:

$$\begin{bmatrix} \hat{\theta}_{r_t} \\ \dot{\hat{\theta}}_{r_t} \end{bmatrix} = A \begin{bmatrix} \hat{\theta}_{r_{t-1}} \\ \dot{\hat{\theta}}_{r_{t-1}} \end{bmatrix} + K_t\Big(\theta_{r_t} - C \begin{bmatrix} \hat{\theta}_{r_{t-1}} \\ \dot{\hat{\theta}}_{r_{t-1}} \end{bmatrix}\Big) \tag{5}$$

being $\begin{bmatrix} \hat{\theta}_{r_t} \\ \dot{\hat{\theta}}_{r_t} \end{bmatrix}$ the current state estimate (i.e., motor reference trajectory and its derivative), $\begin{bmatrix} \hat{\theta}_{r_{t-1}} \\ \dot{\hat{\theta}}_{r_{t-1}} \end{bmatrix}$ the predicted state estimate given past measurements of $\theta_{\mathrm{r}}(t)$ up to time $t-1$, and being $\theta_{\mathrm{r}}(t)$ the current approximated motor reference trajectory. We set the system matrix A, and the output matrix C as follows:

$$A = \begin{bmatrix} 1 & \Delta t \\ 0 & 1 \end{bmatrix}; \; C = \begin{bmatrix} 1 & 0 \end{bmatrix} \tag{6}$$

being Δt the time frame for each update cycle set to 0.01. The term K_t is the Kalman gain and it is used to determine noise characteristics, set by means of a process noise covariance matrix Q and a measurements noise covariance matrix R, such that:

$$K_t = (APC^T)(CPC^T + R)^{-1} \tag{7}$$

where P is the state covariance matrix chosen to minimize the error in the estimate and it is defined as:

$$P = AP_{t-1}A^T + Q \tag{8}$$

$$Q = \begin{bmatrix} 0.02 & 0 \\ 0 & 0.02 \end{bmatrix}; \; R = 0.75 \tag{9}$$

We obtained the actuator's final position reference trajectory, $\theta_{\mathrm{ref}}(t)$, by using a motion mapping method that employed cubic spline interpolation of the sinusoidal profile $\theta_{\mathrm{r}}(t)$.

Low-Level controller A feedback position loop compares the actual position of the motor $\theta_{\mathrm{m}}(t)$ with the reference position $\theta_{\mathrm{ref}}(t)$ extracted from the previous layer. To convert the position error $(\theta_{\mathrm{ref}}(t) - \theta_{\mathrm{m}}(t))$ into motor angular velocity, we used a Proportional-Differential (PD) controller having transfer function:

$$Y(s) = \frac{K_p}{1 + K_d \cdot s} \tag{10}$$

where gains K_p, K_i, and K_d were tuned using the Ziegler-Nichols heuristic method in preliminary trials to accurately follow the desired $\theta_{\mathrm{ref}}(t)$.

Stop condition The stop detection condition is implemented based on the gait speed. The gait speed (s_{gait}) is estimated from the vector norm between $\hat{\theta}(t)$ and $\dot{\hat{\theta}}(t)$ (i.e., polar radius) in the hip phase portrait[1]:

$$s_{gait} = \sqrt{\hat{\theta}(t)^2 + \dot{\hat{\theta}}(t)^2} \tag{11}$$

which is compared to a pre-defined stop threshold experimentally determined on the basis of kinematic sensors noise at rest. Whether the stop condition is met, $\hat{\theta}_r(t)$ is set to zero prior to the application of the Kalman Filter and subsequent interpolation, in order to allow the actuator reference signal to smoothly approach zero thanks to the dynamic behaviour of the filter and thus avoiding abrupt changes and/or discontinuities.

Algorithm 1 *WalkON* Control Algorithm

function HIGH_LEVEL_CONTROLLER($\theta, \dot{\theta}$)
    $\hat{\theta}, \dot{\hat{\theta}} \leftarrow$ NORMALIZEANDCENTER($\theta, \dot{\theta}$)
    $\phi \leftarrow$ CALCULATE_GAIT_PHASE($\hat{\theta}, \dot{\hat{\theta}}$)
    $\theta_r \leftarrow \sin(\phi)$
    return θ_r
end function

function MID_LEVEL_CONTROLLER(θ_r, Δ_t, q, r)
    $A \leftarrow \begin{bmatrix} 1 & \Delta_t \\ 0 & 1 \end{bmatrix}, C \leftarrow \begin{bmatrix} 1 \\ 0 \end{bmatrix}, Q \leftarrow \begin{bmatrix} q & 0 \\ 0 & q \end{bmatrix}, R \leftarrow r$
    current_state $\leftarrow$ KALMAN_FILTER($\theta_{\mathrm{r}}, A, C, Q, R$)
    $\theta_{\mathrm{ref}} \leftarrow$ CUBIC_SPLINE_INTERPOLATION(current_state)
    return θ_{ref}
end function

function LOW_LEVEL_CONTROLLER($\theta_{\mathrm{ref}}, \theta_{\mathrm{m}}$)
    motor_velocity $\leftarrow$ PD_CONTROLLER($\theta_{\mathrm{ref}} - \theta_{\mathrm{m}}$)
    return motor_velocity
end function

function MAIN_CONTROLLER($\theta, \dot{\theta}, \Delta_{\mathrm{t}}, q, r, \theta_{\mathrm{m}}$)
    $\theta_{\mathrm{r}} \leftarrow$ HIGH_LEVEL_CONTROLLER($\theta, \dot{\theta}$)
    $\theta_{\mathrm{ref}} \leftarrow$ MID_LEVEL_CONTROLLER($\theta_{\mathrm{r}}, \Delta_{\mathrm{t}}, q, r$)
    motor_velocity $\leftarrow$ LOW_LEVEL_CONTROLLER($\theta_{\mathrm{ref}}, \theta_{\mathrm{m}}$)
    return motor_velocity
end function

function STOP_CONDITION($\hat{\theta}, \dot{\hat{\theta}}$, stop_threshold)
    $s_{\mathrm{gait}} \leftarrow \sqrt{\hat{\theta}^2 + \dot{\hat{\theta}}^2}$
    if $s_{\mathrm{gait}} <$ stop_threshold **then**
        return True
    else
        return False
    end if
end function

MAIN CODE
while True **do**
    $\theta, \dot{\theta} \leftarrow$ READ_SENSORS
    if not STOP_CONDITION() **then**
        motor_velocity $\leftarrow$ MAIN_CONTROLLER($\theta, \dot{\theta}, \Delta_{\mathrm{t}}, q, r, \theta_{\mathrm{m}}$)
        ACTUATE_MOTOR(motor_velocity)
    else
        STOP_MOTOR
    end if
end while

WalkON design: a comparative study on two hardware configurations in young adults hiking

WalkON was conceived primarily with the objective of capitalizing on lightweight design, efficient weight distribution, and a comfortable textile interface. In reference to the first two aspects, in the current literature, an ongoing debate exists between two different design configurations for wearable assistive robotic devices[3]: underactuated systems (with fewer motors per assisted degrees of freedom)[4,5,6] and fully-actuated systems (with one motor per assisted degree of freedom)[7,8,9]. Underactuated assistive devices have a simpler and lighter design due to fewer motors, making them energy-efficient and capable of leveraging the synergistic nature of human movements. In contrast, fully-actuated systems offer precise and independent joint control, providing adaptability to user needs and environmental conditions, broadening their application range.

Investigated hardware configurations

To investigate the best actuation approach to assist hip flexion in outdoor unstructured walking, we developed two distinct mechanical configurations for *WalkON* (Fig. 2) and conducted a comparative study with young adults on the hiking trail (Fig. 3). Comparison between the biomechanical effects of these two hardware configurations is the outcome of this study and was meant to determine the strategy offering greater metabolic benefits.

Both *WalkON* designs share primary hardware components and the controller, but their mechanical actuation principle sets them apart: one is an underactuated system, while the other is fully-actuated. The two different designs will be referred to in the following as *WalkON -U* and *WalkON -F* to indicate their underactuated and fully-actuated nature respectively.

Specifically, *WalkON -U* employs a single centrally located motor (AK80-6, 12Nm peak torque, T-MOTOR, China) equipped with a double-layer pulley (diameter 78mm). It utilizes centrally back-located weight distribution and symmetrically couples the two legs in a single assistance profile, with the motor alternately pulling and releasing the two artificial tendons based on the contralateral leg's gait phase shift. On the other hand, *WalkON -F* is a fully-actuated system with two motors (AK60-6, 9Nm peak torque, T-Motor, China), each wrapping up the artificial tendon of the respective leg on spools with a diameter of 35mm. This design allows independence between assisted legs, enabling adjustments in the assistance profile to accommodate more complex movements and a broader range of motion. Each device weighs less than 3kg, with *WalkON -U* weighing 2.77 kg and *WalkON -F* weighing 2.93 kg. Actuation and electronics account for the 5% difference in weight between the two systems and comprise most of the device's total weight. These components are located on the backside of the waist, approximately at the level of the user's center of mass, to minimize the impact of the extra mass on the metabolic energy expenditure during walking[10]. Both *WalkON* configurations are represented in Fig. 2.

Controller generalization to hardware configuration

The model outlined in the previous section for controlling tendon displacements during walking represents a general framework applicable to any tendon-driven system intended to assist walking, and can be generalized to the hardware configuration. In this comparative study, we preserved the core of the controller for both *WalkON -U*, the underactuated system, and *WalkON -F*, the fully actuated systems, in order to allow comparison of results between the two devices. We solely adjusted the inputs and outputs of the controller to

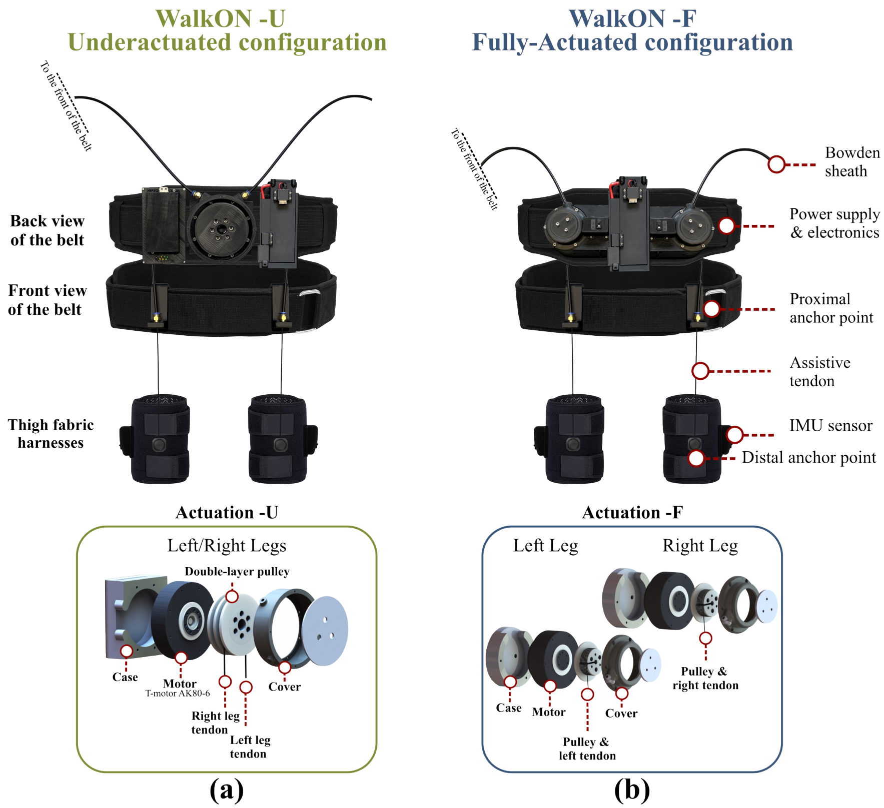

Fig. 2 ***WalkON configurations*** **(a)** *WalkON -U* features s single centrally located motor and a double layer pulley wrapping up the two artificial assistive tendonds in opposite directions. **(b)** *WalkON -F* features one actuator per leg such that the two artificial assistive tendons remain independent.

account for the specific underactuated or fully-actuated nature of the device as follows.

WalkON -U To control the underactuated system, the inter-limb flexion angle obtained from the two IMUs is used as the input signal to the controller. This angle represents the difference between the right and left hip angles and results in a symmetrical sinusoidal-like trend, where positive values correspond to the displacement of the right leg, and negative values indicate the displacement of the left leg. Accordingly, the controller generates a motion inversion of the motor that is symmetrical, such that during the flexion of the right leg, the right tendon is pulled while the left tendon is released by the same amount, and vice versa during the flexion of the left leg.

WalkON -F In the case of a fully-actuated system with one motor per leg, the control strategy is independent between the two legs and uses the respective hip flexion angle as the input signal. In this hardware configuration, the controller output is an asymmetrical motor reference trajectory that wraps up the tendon during hip flexion to provide assistance and releases it to a lesser extent as the hip extends.

Results of the comparative study

The primary aim of this comparative study is to evaluate the impact of two distinct hardware configurations in order to determine the most effective actuation strategy for assisting outdoor walking.

To achieve this objective, the seven young adults (age 25.43 ± 2.23 years, height 172.57 ± 12.42 cm, and weight 67.57 ± 13.06 kg) performing the technology assessment of *WalkON* on the hiking-like trails, were instructed to walk at their preferred speed while utilizing also the underactuated system, marking a third condition in addition to those detailed in the main text. Hereafter, the three conditions are referred to as: *No Assistance* (system turned off), with assistance from *WalkON -U* (underactuated configuration), and with assistance from *WalkON -F* (fully-actuated configuration).

After completing the 500m uphill walking (Fig. 3, Philosophenweg, Heidelberg, 49°24'55.1"N 8°42'00.9"E), each participant retraced the same path in the opposite direction, going downhill. The walking distance for each condition of the study accounted then for a total of 1 km walked. Results are presented in the following separately for the the uphill and downhill sections. However, results during downhill walking are hereby included for completeness

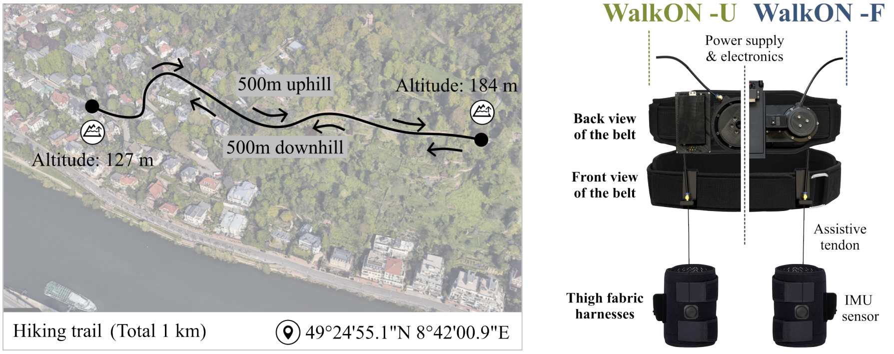

Fig. 3 The task involved walking along a steep and winding trail (total distance 1km: 500m uphill/500m downhill). Young adults walked at their preferred pace being unassisted (*No Assistance*), utilizing the *WalkON -U* (green), and the *WalkON -F* (navy).

of evaluation, as assistance provided by *WalkON* for hip flexion is less significant during downhill tracks. This is because the swinging leg does not need to be lifted as high during downhill walking for ground clearance [11]. The aim of retracing the path downhill is to demonstrate that the assistive system and its weight do not impede motion or impose a metabolic burden.

The different conditions were tested on separate days to minimize any fatigue-related effects. The metabolic cost of transport, the hip joint motion, and the sense of agency were assessed as described in the main text.

Uphill hiking

Using *WalkON -U*, the metabolic demand of traversing the outdoor uphill trail was significantly reduced by an average of $-13.19 \pm 4.38\%$ (mean $\pm$ s.e.m., n $= 7$, p $= 0.007$), while using *WalkON -F* it was reduced by $-17.04 \pm 3.21\%$ (p < 0.001) (Fig. 4-(a, b)). The linear walking velocity (Fig. 4-(c)) did not show significant differences across conditions, although there was a noticeable trend a -6% with *WalkON -U* and a $+5\%$ increase with *WalkON -F* compared to the *No Assistance* condition.

Wearing *WalkON* did not impose any restrictions on the motion of the hip joint (Fig. 4-(d, e)). In the absence of assistance (*No Assistance*), the average

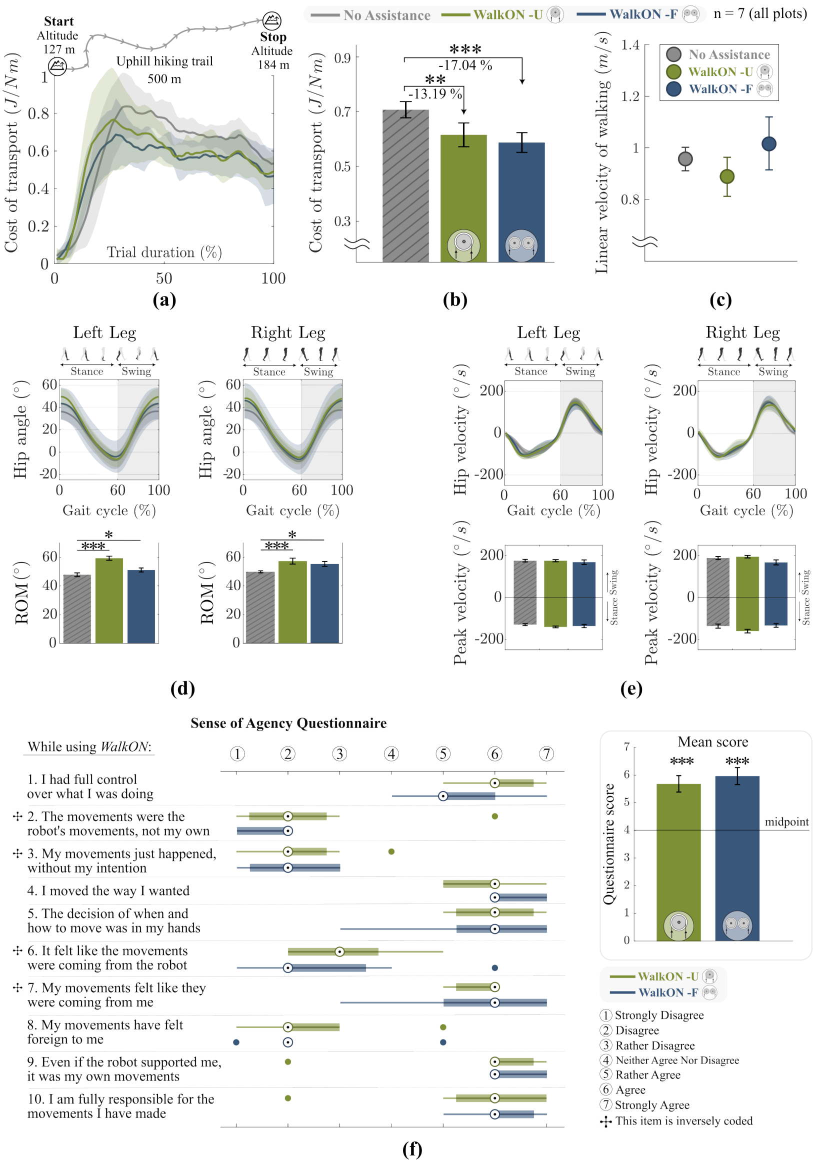

Fig. 4 Uphill outdoor walking task results for young adults (a) Cost of transport timeseries averaged across subjects normalized according to trial duration. **(b)** Mean cost of transport significantly reduced when using *WalkON*, with higher savings for *WalkON -F*. **(c)** The preferred walking speed along the trail was unaltered when using *WalkON*. **(d)** The hip range of motion exhibited a significant increase with either *WalkON -U* and *WalkON -F* compared to the *No Assistance* condition. **(e)** There were no significant variations in hip velocity peaks with both *WalkON* configurations compared to *No Assistance*. **(f)** The sense of agency assessment for young adults demonstrated that users perceived strong sense of control when using *WalkON* in both configurations. Grey colors indicate *No Assistance*, green *WalkON -U*, and navy *WalkON -F*. *p $<$ 0.05, ** p $<$ 0.01, and p $<$ 0.001.

range of motion across both legs and subjects was 48.82° ± 0.68° (mean ± s.e.m.). This range significantly increased to 58.40° ± 1.50° when utilizing *WalkON -U* and to 53.21° ± 1.32° with *WalkON -F*. These findings reflect an average increase of +19.69 ± 3.04% ($n = 7$, $p < 0.001$) and +9.08 ± 2.83% ($p < 0.05$) for the two robotic shorts configurations compared to the *No Assistance* condition (Fig. 4-(d)). The assistance provided by the device did not yield any significant alterations in hip peak velocities throughout the gait cycle, (Fig. 4-(e)).

For both *WalkON -U* and *WalkON -F*, young adults consistently indicated that their sense of agency remained almost intact during system usage (Fig. 4-(f)), reporting a mean score of 5.67 ± 0.30 (mean ± s.e.m.) with *WalkON -U* and 5.93 ± 0.31 with *WalkON -F*. Both conditions resulted significantly higher (p-value < 0.001) compared to a midpoint of 4 on the Likert scale, indicating neither agreement nor disagreement with the statements.

Downhill hiking

The use of *WalkON* downhill did not significantly influenced the metabolic cost of transport (Fig. 5-(a, b)). The linear walking velocity exhibited a significant decrease with *WalkON -U* ($n = 7$, $p = 0.005$), but showed no significant change with *WalkON -F* (Fig. 5-(c)).

WalkON facilitated unrestricted, natural hip motion, as indicated by a significant ROM increase with both *WalkON* configurations. Specifically, in the *No Assistance* condition the average ROM across legs and participants was 34.85° ± 1.02°, which increased to 41.55° ± 1.20° with *WalkON -U* (+19.69 ± 4.19%, $p < 0.05$), and to 38.92° ± 2.24° with *WalkON -F* (+12.16 ± 6.89%, $p < 0.05$). Hip peak velocities remained unaffected by the devices.

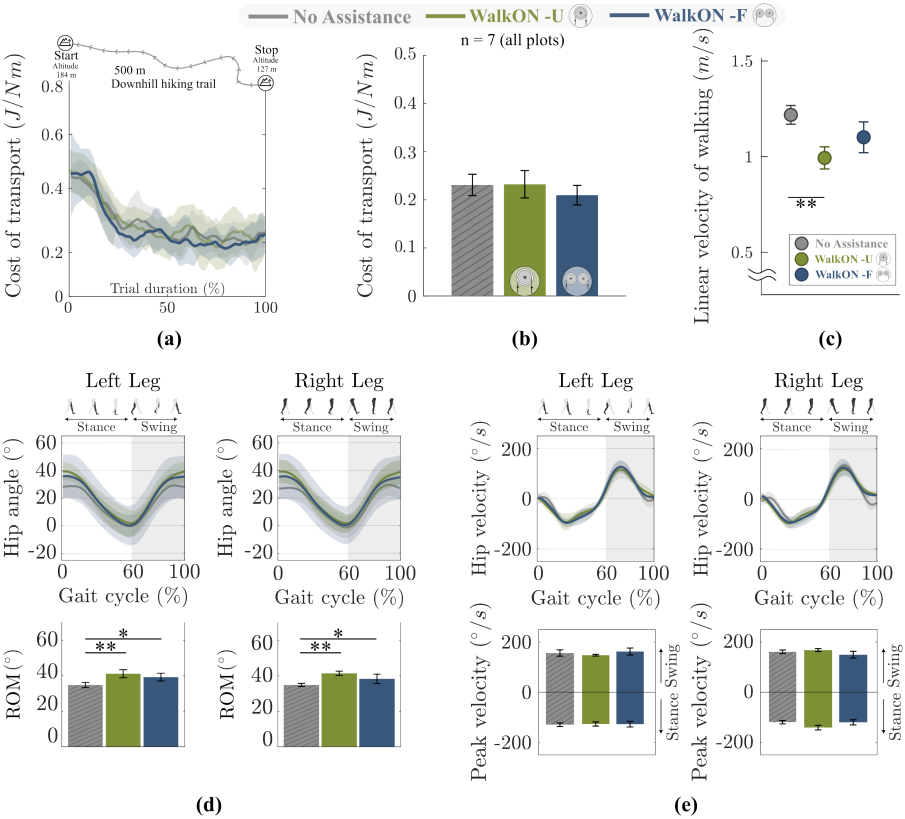

Fig. 5 Downhill outdoor walking results for young adults The task involved retracing back the 500m uphill hiking trail. Young adults walked at their preferred speed without assistance (*No Assistance* in grey), utilizing the *WalkON -U* device (in green), and the *WalkON -F* device (in navy). **(a, b)** The use of *WalkON* downhill did not impose a metabolic burden with either configurations. **(c)** The linear walking velocity exhibited a significant decrease with *WalkON -U*, but showed no significant change with *WalkON -F*. **(d, e)** The range of motion (ROM) of the hip joint significantly increased. Hip peak velocities remained unaffected by the devices. *$p < 0.05$, ** $p < 0.01$.

Selection of the most efficient *WalkON* configuration

In this comparative study involving young adults, the utilization of the fully-actuated version of *WalkON* (referred to as *WalkON -F*) led to higher metabolic efficiency uphill, achieving a 17.04% saving, with individual outcomes varying from 7.44% to 33.64%. On the other hand, the system in its underactuated configuration, designated as *WalkON -U*, yielded lower results, although it still enabled an average saving of 13.19%.

When assessing the kinematic effects, it was observed that *WalkON -U* induced a more substantial increase in the physiological range of motion, both uphill and downhill, while *WalkON -F* induced comparatively more modest changes in natural motion. The psycho-physical evaluation results, measured in terms of the sense of agency, showed no differences between the two configurations, yet higher scores were reported with *WalkON -F*.

It is conceivable that the superior performance of *WalkON -F* can be attributed to its ability to independently and accurately control each leg. This capability may enable a finer level of synchronization with the user's natural walking pattern, especially in situations where the two legs need to move asymmetrically, as is often the case on sloped or uneven terrains. This characteristic likely played a crucial role, particularly on challenging terrains like the selected hiking path, where the two legs may have needed distinct movements to adjust to variations in slope and ground contours.

Given the enhanced performance of *WalkON -F* on the evaluated metrics, we have chosen this design configuration as the preferred option and final design of the assistive system to be tested with older adults.

References

[1] David Quintero, Daniel J Lambert, Dario J Villarreal, and Robert D Gregg. Real-time continuous gait phase and speed estimation from a single sensor. In *2017 IEEE Conference on Control Technology and Applications (CCTA)*, pages 847–852. IEEE, 2017.

[2] Greg Welch, Gary Bishop, et al. An introduction to the kalman filter. 1995.

[3] Michele Xiloyannis, Eugenio Annese, Marco Canesi, Anil Kodiyan, Antonio Bicchi, Silvestro Micera, Arash Ajoudani, and Lorenzo Masia. Design and validation of a modular one-to-many actuator for a soft wearable exosuit. *Frontiers in neurorobotics*, 13:39, 2019.

[4] Fausto A Panizzolo, Ignacio Galiana, Alan T Asbeck, Christopher Siviy, Kai Schmidt, Kenneth G Holt, and Conor J Walsh. A biologically-inspired multi-joint soft exosuit that can reduce the energy cost of loaded walking. *Journal of neuroengineering and rehabilitation*, 13(1):1–14, 2016.

[5] Florian Leander Haufe, Kai Schmidt, Jaime Enrique Duarte, Peter Wolf, Robert Riener, and Michele Xiloyannis. Activity-based training with the myosuit: a safety and feasibility study across diverse gait disorders. *Journal of neuroengineering and rehabilitation*, 17:1–11, 2020.

[6] Enrica Tricomi, Nicola Lotti, Francesco Missiroli, Xiaohui Zhang, Michele Xiloyannis, Thomas Müller, Simona Crea, Emese Papp, Jens Krzywinski, Nicola Vitiello, et al. Underactuated soft hip exosuit based on adaptive oscillators to assist human locomotion. *IEEE Robotics and Automation Letters*, 7(2):936–943, 2021.

[7] Jinsoo Kim, Giuk Lee, Roman Heimgartner, Dheepak Arumukhom Revi, Nikos Karavas, Danielle Nathanson, Ignacio Galiana, Asa Eckert-Erdheim, Patrick Murphy, David Perry, et al. Reducing the metabolic

rate of walking and running with a versatile, portable exosuit. *Science*, 365(6454):668–672, 2019.

[8] Alan T Asbeck, Kai Schmidt, and Conor J Walsh. Soft exosuit for hip assistance. *Robotics and Autonomous Systems*, 73:102–110, 2015.

[9] Enrica Tricomi, Mirko Mossini, Francesco Missiroli, Nicola Lotti, Xiaohui Zhang, Michele Xiloyannis, Loris Roveda, and Lorenzo Masia. Environment-based assistance modulation for a hip exosuit via computer vision. *IEEE Robotics and Automation Letters*, 2023.

[10] MJ Myers and K Steudel. Effect of limb mass and its distribution on the energetic cost of running. *Journal of Experimental biology*, 116(1):363–373, 1985.

[11] M Kuster, S Sakurai, and GA Wood. Kinematic and kinetic comparison of downhill and level walking. *Clinical biomechanics*, 10(2):79–84, 1995.